Evaluation of Performance of FACTS based Phase Imbalance Schemes for Damping Torsional Oscillations and Power Swings

Mahipalsinh C. Chudasama, S. R. Joshi and A. M. Kulkarni

***Abstract*—Recent investigations have focused on the use of active phase imbalance schemes using series connected FACTS devices for subsynchronous resonance (SSR) and power swing damping. This paper compares the effectiveness of TCSC and SSSC based single phase compensation schemes with the corresponding three phase schemes. Controllability of swing modes as well as torsional modes is compared by using a simplified, dynamic phasor based expression of the linearized electrical torque of a synchronous machine connected to a compensated transmission line. The analysis and simulation studies show that a single phase scheme is unlikely to be an attractive alternative to a three phase scheme from a cost and sizing perspective.**

***Index Terms*—SSR Mitigation, Phase imbalance, Dynamic phasors, TCSC, SSSC**

I. Introduction

Compensation of transmission line reactance using fixed capacitors is an economical and effective technique to enhance the power transfer capability of transmission lines [1]. However, such systems are prone to adverse interaction with the turbine-generator shafts due to the Sub-Synchronous Resonance (SSR) phenomenon [2]. The use of controlled series compensation - Thyristor Controlled Series Compensator (TCSC) or Static Synchronous Series Compensator (SSSC) [1], [3] in conjunction with fixed capacitor compensation, is one of the possible solutions to the problem. The effectiveness of this solution depends on the relative sizing of fixed capacitor and the TCSC/SSSC based variable compensation, and the control strategy used for the control of the TCSC/SSSC.

It has been conjectured that introducing phase imbalance in a series compensation scheme can be an effective countermeasure for SSR [4], [5]. Although the overall steady state compensation is equal in all phases, it is achieved via different combinations of reactors and capacitors in the three phases (*passive* phase imbalance scheme). A recent study of a passive imbalance scheme [6] indicates that it can not be a general SSR countermeasure.

An alternative is to use different relative sizes of fixed capacitors and TCSC/SSSC based controlled compensation in the three phases, while keeping the overall steady state compensation same in all the phases. The schematic of such schemes are shown in Figs. 1. Recent investigations have focused on the use of these *active* phase imbalance schemes not only for SSR mitigation but also for power swing damping [7]–[9]. It is understood that if the critical torsional modes or the low frequency swing modes are controllable by varying balanced or unbalanced injected reactance or voltage, then it should be possible to improve their damping by appropriate control. However, the actual effectiveness depends on the magnitude of modal controllability - which determines the amount of control effort required to get a certain damping performance. The control effort is correlated to the dynamical

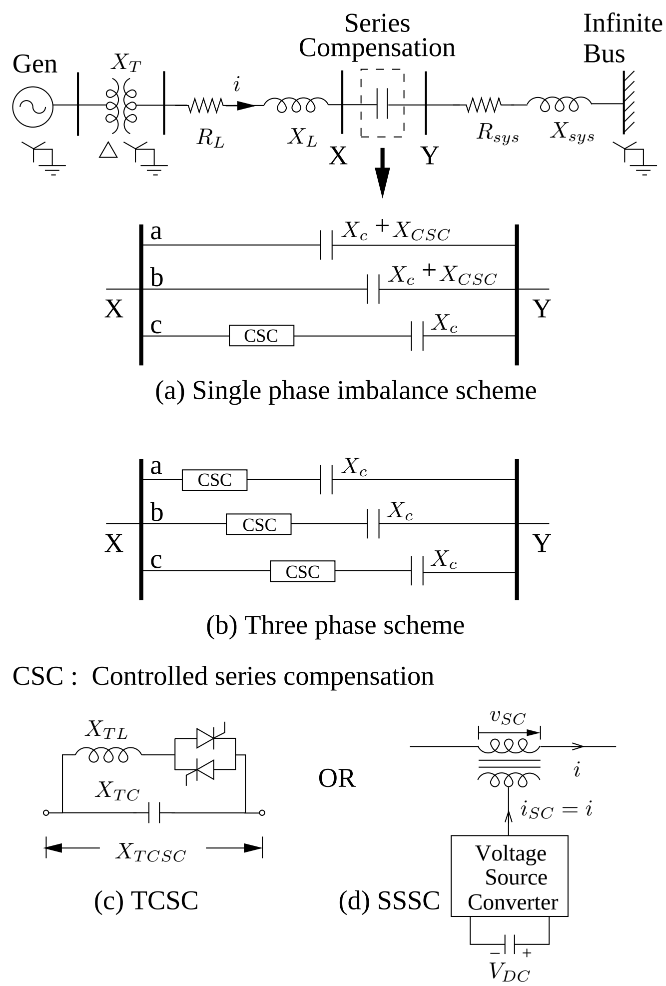

Fig. 1. Single line diagram of a series compensated system

M. C. Chudasama and A. M. Kulkarni are with Department of Electrical Engineering, Indian Institute of Technology Bombay, Powai, Mumbai-400076, India. (e-mail of corresponding author: mahipal75@iitb.ac.in).

S. R. Joshi is with Department of Electrical Engineering, Government Engineering College, Surat-395001, India. (e-mail: sanjayrjoshi@gmail.com)

Paper submitted to the International Conference on Power Systems Transients (IPST2011) in Delft, the Netherlands June 14-17, 2011.

range of the controllable device and its cost.

This paper presents the application of dynamic phasor analysis and digital simulation to evaluate controllable phase imbalance schemes and compare them with balanced schemes. Modal controllability is compared by evaluating the simplified expression of linearized electrical torque of a synchronous machine. Not unexpectedly, it is seen that the controllability for a single phase scheme is exactly one-third of that in the three phase case. This is true when network transients are considered (SSR study) as well as when they are neglected (power swing study).

To validate this analysis using simulation, we first consider the SSR performance of constant firing angle control for TCSC and constant reactive voltage injection for a SSSC. Here, SSR avoidance is by the detuning or passive damping ability of these devices. The simulation studies confirm that the variable compensation size requirement to stabilize both torsional and swing modes is much larger in the single phase case. Since it is better to design specific damping controllers in order to utilize the devices better, a comparison with the use of damping controllers is also carried out. It is seen that good damping is achieved with reasonable gains and dynamic range for the three phase balanced case, while it is difficult to achieve the same for single phase schemes. The analysis and simulation study show that a single phase scheme is unlikely to be an attractive alternative to a three phase scheme from a cost and sizing perspective.

The paper is organized as follows. An introduction to dynamic phasor models is given in section II. Derivation of controllability factors for a Single Machine Infinite Bus (SMIB) system with simplified models is shown in the next section. Digital simulation results with detailed models are presented in section IV.

II. Dynamic phasor modeling

The aim of the analysis presented in the next two sections is to obtain analytical expressions for electrical torque using a simplified model of a synchronous machine and a compensated transmission line. Since unbalanced compensation is considered in the analysis it is convenient to use dynamic phasor modeling because it yields a time-invariant model of the system. We first present the essentials of dynamic phasor modeling which is followed by the simplified analysis.

Any periodic waveform (possibly complex) can be represented in terms of the complex Fourier coefficients as given in the following:

$$x(\tau) = \sum_{k=-\infty}^{\infty} \langle x \rangle_k(t) e^{jk\omega_s \tau} \quad \tau \in (t-T, t] \tag{1}$$

where $\omega_s = \frac{2\pi}{T}$.

Dynamic phasors are the state variables in the dynamic phasor based models. $\langle x \rangle_k$ represents the k^{th} dynamic phasor of the instantaneous signal $x(t)$ and can be computed as follows:

$$\langle x \rangle_k(t) = \frac{1}{T}\int_{t-T}^{t} x(\tau) e^{-jk\omega_s \tau} d\tau \tag{2}$$

The derivative of the dynamic phasor is given by [10]:

$$\frac{d\langle x \rangle_k}{dt} = \left\langle \frac{dx}{dt} \right\rangle_k - jk\omega_s \langle x \rangle_k \tag{3}$$

Note that if $x(t)$ is periodic with a period T, then the dynamic phasor $\langle x \rangle_k(t)$ is a constant.

The basic equations in "abc" variables are transformed to positive, negative and zeros sequence variables using following transformation.

$$f_{pnz} = \begin{bmatrix} f_p \\ f_n \\ f_z \end{bmatrix} = \frac{1}{\sqrt{3}} \begin{bmatrix} 1 & a & a^2 \\ 1 & a^2 & a \\ 1 & 1 & 1 \end{bmatrix} \begin{bmatrix} f_a \\ f_b \\ f_c \end{bmatrix}$$

where, $a = e^{j2\pi/3} = 1\angle 120^0$.

The equations in terms of sequence variables are then converted to dynamic phasor form using (2) and (3).

III. Simplified Analysis

Before proceeding for a digital simulation using detailed models, we carry out a simplified analysis using a simple (voltage behind reactance) generator model.

Torsional and electro-mechanical modal damping can be evaluated by considering the linearized second order differential equation for modal rotor angle deviation [2]:

$$\frac{2H_m}{\omega_B}\frac{\mathrm{d}^2\langle \Delta\delta_m \rangle_0}{\mathrm{d}t^2} = -\langle \Delta T_e \rangle_0 \tag{4}$$

where H_m is the modal inertia, ω_B is the base speed, δ_m is the modal rotor angle as defined in [2], and ΔT_e is the linearized electrical torque. Mechanical torque input is assumed to be constant.

If the mode shapes (eigenvectors) for these modes are assumed to be unchanged due to the compensation, and damping is low, then the damping and synchronizing effects can be evaluated by obtaining the transfer function between the linearized electrical torque and the generator rotor angle / speed deviations [2] at the modal frequencies (damping and synchronizing torque coefficients). In addition, the transfer function between the linearized electrical torque and the controlled variable (for FACTS devices) will give us the modal controllability with the use of these devices.

Therefore our aim is to obtain *linearized* expressions of electrical torque under the following circumstances:

1) Network Transients neglected (for study of low frequency power swings) and reactance modulation.
2) Network Transients considered (for SSR studies) and
   a) With series voltage modulation - to understand the effect of a SSSC
   b) With modulation of current through a capacitor - to understand the effect of a TCSC

The analysis is facilitated by the time invariant nature of the balanced/unbalanced network equations when they are formulated using dynamic phasors. The derivation follows the approach given in [6]. An outline of it is presented below.

The linearized torque and "internal" voltage of the generator are given by [2]:

$$\Delta T_e = E'\Delta i_Q$$

$$\Delta e_Q + j\Delta e_D = \Delta(\frac{\omega}{\omega_B}E'\angle\delta) = \frac{E'}{\omega_B}\Delta\omega + jE'\Delta\delta$$

(e_D, e_Q, i_D, i_Q) are the generator internal voltage and current components in the synchronously rotating D-Q frame of reference. $\omega E'/\omega_B$ is the magnitude of the voltage behind the generator reactance.

It is assumed here, for simplicity, that the generator is operating at no load, i.e., the quiescent currents of the generator (i_{D0}, i_{Q0}) and the quiescent value of δ are zero. The quiescent frequency is equal to ω_s which is also equal to the base frequency ω_B. Therefore:

$$\langle \Delta T_e \rangle_0 = E' \langle \Delta i_Q \rangle_0; \quad \langle \Delta\delta \rangle_0 = \frac{1}{s} \langle \Delta\omega \rangle_0$$

$$\langle \Delta e_D \rangle_0 = E' \langle \Delta\delta \rangle_0; \quad \langle \Delta e_Q \rangle_0 = \frac{E'}{\omega_B} \langle \Delta\omega \rangle_0$$

We can rewrite this in terms of dynamic phasors of sequence components by using the relationships between the $D-Q$ and $p-n$ dynamic phasors - see [6]:

$$\langle e_p \rangle_{1R} = \frac{1}{\sqrt{2}} \langle e_D \rangle_0 \quad \text{and} \quad \langle e_p \rangle_{1I} = -\frac{1}{\sqrt{2}} \langle e_Q \rangle_0 \tag{5}$$

$$\langle i_p \rangle_{1R} = \frac{1}{\sqrt{2}} \langle i_D \rangle_0 \quad \text{and} \quad \langle i_p \rangle_{1I} = -\frac{1}{\sqrt{2}} \langle i_Q \rangle_0 \tag{6}$$

where the subscripts R and I denote real and imaginary components. The currents and voltages are related by the equations of a network. For a series compensated RLC network, the equations are given by [6]:

$$\begin{aligned} \frac{d}{dt} \langle i_{pnz} \rangle_1 = & -\omega_B B_L R_m \langle i_{pnz} \rangle_1 - \omega_B B_L \langle v_{c\ pnz} \rangle_1 \\ & + \omega_B B_L \langle E_{pnz} \rangle_1 - j\omega_B \langle i_{pnz} \rangle_1 \\ & (\text{where, } \ E_{pnz} = e_{pnz} - e_{B\ pnz}) \end{aligned} \tag{7}$$

$$\frac{d}{dt} \langle v_{c\ pnz} \rangle_1 = \omega_B X_C \langle i_{pnz} \rangle_1 - j\omega_B \langle v_{c\ pnz} \rangle_1 \tag{8}$$

where i and v_c represent line current and capacitor voltage respectively. e and e_B are the instantaneous values of the generator voltage behind reactance and infinite bus voltage respectively. ω_B is the rated (base speed) in rad/s. Subscript '1' is used to represent the dynamic phasors corresponding to fundamental frequency ($k = 1$).

Moreover,

$$R_m = \begin{bmatrix} R_p & 0 & 0 \\ 0 & R_p & 0 \\ 0 & 0 & R_z \end{bmatrix}; \quad X_C = P^{-1} \begin{bmatrix} X_{ca} & 0 & 0 \\ 0 & X_{cb} & 0 \\ 0 & 0 & X_{cc} \end{bmatrix} P$$

$$B_L = \begin{bmatrix} \frac{1}{X_p} & 0 & 0 \\ 0 & \frac{1}{X_p} & 0 \\ 0 & 0 & \frac{1}{X_z} \end{bmatrix}; \quad P = \frac{1}{\sqrt{3}} \begin{bmatrix} 1 & 1 & 1 \\ a^2 & a & 1 \\ a & a^2 & 1 \end{bmatrix}$$

where, X_p and X_z are the positive sequence and zero sequence reactances of the line, which include the generator sub-transient reactance. R_p and R_z are positive sequence and zero sequence resistances. X_{ca}, X_{cb} and X_{cc} are the capacitive reactances of different phases of the RLC series network.

If network equations in abc variables are linear time-invariant as above, then there is no coupling between dynamic phasors corresponding to various k. However, with imbalance there is coupling between the p, n and z variables for a given k.

Note that it is adequate to consider only $k = 0$ for the mechanical variables and $k = \pm 1$ for the electrical variables, since these dynamic phasors are decoupled from those corresponding to other values of k, due to the use of the simplified generator model.

A. Series Reactance Modulation: Network transients neglected

For the study of low frequency power swings, we can neglect the network transients i.e. $\frac{d}{dt} \langle i_{pnz} \rangle_1 = 0$ and $\frac{d}{dt} \langle v_{c\ pnz} \rangle_1 = 0$. The network is in quasi-sinusoidal steady state and the variable compensation (either by a TCSC or by SSSC) can be represented by equivalent reactance modulation. In such a case the linearized electrical torque expressions are given below.

1) Single Phase Imbalance Case
The capacitive reactance of only one phase is variable, i.e. $X_{ca} = X_{cb} = X_c$ and $X_{cc} = X_c + \Delta x$.

$$\begin{aligned} \langle \Delta T_e \rangle_0 = & \frac{E'}{3} \begin{Bmatrix} 2G_p B_p (1 - E' \cos\delta_0) \\ -(G_p^2 - B_p^2) E' \sin\delta_0 \end{Bmatrix} \Delta x \\ & + G_p E'^2 \frac{\langle \Delta\omega \rangle_0}{\omega_B} - B_p E'^2 \langle \Delta\delta \rangle_0 \end{aligned} \tag{9}$$

where,

$$G_p = \frac{R_p}{R_p^2 + (X_p - X_c)^2}; \ B_p = \frac{-(X_p - X_c)}{R_p^2 + (X_p - X_c)^2}$$

δ, and ω are the angle and speed of the generator rotor mass.

2) Balanced Case
In this case equal variations are applied to capacitive reactances in all phases. i.e. $X_{ca} = X_{cb} = X_{cc} = X_c + \Delta x$ which gives,

$$\begin{aligned} \langle \Delta T_e \rangle_0 = & E' \begin{Bmatrix} 2G_p B_p (1 - E' \cos\delta_0) \\ -(G_p^2 - B_p^2) E' \sin\delta_0 \end{Bmatrix} \Delta x \\ & + G_p E'^2 \frac{\langle \Delta\omega \rangle_0}{\omega_B} - B_p E'^2 \langle \Delta\delta \rangle_0 \end{aligned} \tag{10}$$

It is observed from (9) and (10) that the controllability of single phase imbalance scheme is one third of balanced three phase scheme.

B. Analysis with TCSC: Network transients considered

For SSR analysis one has to consider network and stator flux transients. In order to simplify the analysis, the TCR branch of a TCSC is modelled as a controlled current source. The single line diagram for the system with a TCSC is shown in Fig. 2. The dynamic phasor model for the system shown is given below.

$$\begin{aligned} \frac{d}{dt} \langle i_{pnz} \rangle_1 = & -\omega_B B_L R_m \langle i_{pnz} \rangle_1 + \omega_B B_L \langle E_{pnz} \rangle_1 \\ & -\omega_B B_L \langle v_{c\ pnz} + v_{c1\ pnz} \rangle_1 - j\omega_B \langle i_{pnz} \rangle_1 \end{aligned} \tag{11}$$

$$\frac{d}{dt} \langle v_{c\ pnz} \rangle_1 = \omega_B X_C \langle i_{pnz} \rangle_1 - j\omega_B \langle v_{c\ pnz} \rangle_1 \tag{12}$$

$$\begin{aligned} \frac{d}{dt} \langle v_{c1\ pnz} \rangle_1 = & \ \omega_B X_{C1} \langle i_{pnz} - i_{TC\ pnz} \rangle_1 \\ & -j\omega_B \langle v_{c1\ pnz} \rangle_1 \end{aligned} \tag{13}$$

If the transfer function of the electrical torque is evalu-

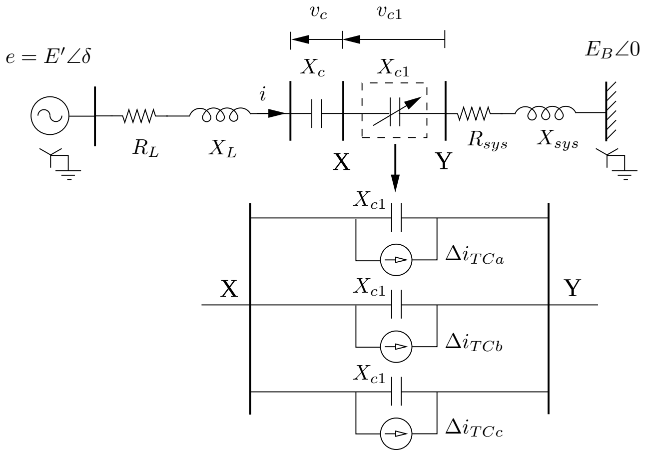

Fig. 2. Series compensated SMIB system with TCSC

ated for a torsional mode frequency which is nearest to the subsynchronous network frequency (imaginary part of λ as given below), then the transfer function is dominated by the following term :

$$\begin{aligned}\langle \Delta T_e \rangle_0 (j\Omega) \approx & -\frac{E'^2 \omega_B (R_p + jX'_p)}{4X_p X'_p (j\Omega - \lambda)} \langle \Delta\delta \rangle_0 (j\Omega) \\ & -\frac{jE'^2 (R_p + jX'_p)}{4X_p X'_p (j\Omega - \lambda)} \langle \Delta\omega \rangle_0 (j\Omega) \\ & +\frac{\sqrt{2} E' \omega_B X_{c1} (R_p^2 + X'^2_p)}{8X_p X'_p (X_c + X_{c1})(j\Omega - \lambda)} \langle \Delta i_{TCp} \rangle_1^* (j\Omega)\end{aligned} \tag{14}$$

where, $X'_p = \sqrt{4X_p(X_c + X_{c1}) - R_p^2}$

$$\lambda = \frac{\omega_B}{2X_p} \left\{ -R_p + j(2X_p - X'_p) \right\}$$

1) Single Phase Imbalance Case
   In this case we consider perturbation in TCR branch current of only one phase (i.e. $\Delta i_{TCa} = \Delta I \sin(\omega_B t + \phi)$, $\Delta i_{TCb} = \Delta i_{TCc} = 0$), which results into

$$\langle \Delta i_{TCp} \rangle_1 (j\Omega) = \frac{\Delta I}{2\sqrt{3}j} e^{j\phi}$$

2) Balanced Case
   Here we consider balanced three phase perturbation in TCR branch currents (i.e. $\Delta i_{TCa} = \Delta I \sin(\omega_B t + \phi)$, $\Delta i_{TCb} = \Delta I \sin(\omega_B t - 2\pi/3 + \phi)$ and $\Delta i_{TCc} = \Delta I \sin(\omega_B t + 2\pi/3 + \phi)$). This scheme has,

$$\langle \Delta i_{TCp} \rangle_1 (j\Omega) = \frac{\sqrt{3}\Delta I}{2j} e^{j\phi}$$

By substituting these results in (14) we can conclude that controllability of single phase imbalance scheme is, again, one third of that for the balanced scheme.

C. Analysis with SSSC (Network transients considered)

Static synchronous series compensator (SSSC) is modeled as a controlled voltage source in series with the transmission line. Single line diagram for the series compensated system with SSSC is shown in Fig. 3. The dynamic phasor model for this system is:

$$\begin{aligned}\frac{d}{dt}\langle i_{pnz} \rangle_1 = & -\omega_B B_L R_m \langle i_{pnz} \rangle_1 + \omega_B B_L \langle E_{pnz} \rangle_1 \\ & -\omega_B B_L \langle v_{c\ pnz} + v_{SC\ pnz} \rangle_1 - j\omega_B \langle i_{pnz} \rangle_1\end{aligned} \tag{15}$$

$$\frac{d}{dt}\langle v_{c\ pnz} \rangle_1 = \omega_B X_C \langle i_{pnz} \rangle_1 - j\omega_B \langle v_{c\ pnz} \rangle_1 \tag{16}$$

Applying same procedure as in the previous case,

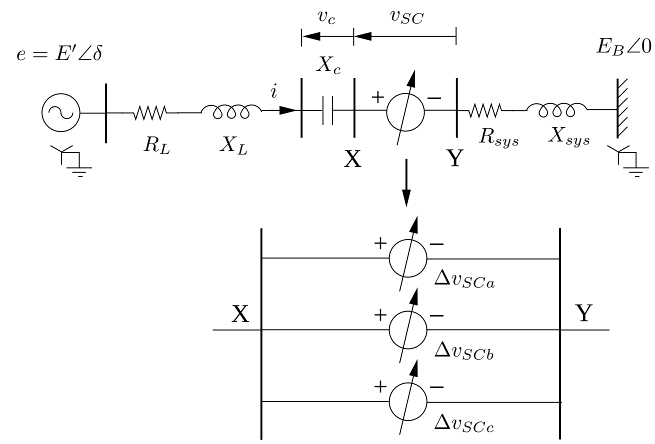

Fig. 3. Series compensated SMIB system with SSSC

$$\begin{aligned}\langle \Delta T_e \rangle_0 (j\Omega) \approx & -\frac{E'^2 \omega_B (R_p + jX''_p)}{4X_p X''_p (j\Omega - \lambda_1)} \langle \Delta\delta \rangle_0 (j\Omega) \\ & -\frac{jE'^2 (R_p + jX''_p)}{4X_p X''_p (j\Omega - \lambda_1)} \langle \Delta\omega \rangle_0 (j\Omega) \\ & +\frac{\sqrt{2} E' \omega_B (R_p + jX''_p)}{4X_p X''_p (j\Omega - \lambda_1)} \langle \Delta v_{SCp} \rangle_1^* (j\Omega)\end{aligned} \tag{17}$$

where, $X''_p = \sqrt{4X_p X_c - R_p^2}$

$$\lambda_1 = \frac{\omega_B}{2X_p} \left\{ -R_p + j(2X_p - X''_p) \right\}$$

1) Single Phase Imbalance Case
   In this case we consider perturbation in SSSC injected voltage of only one phase (i.e. $\Delta v_{SCa} = \Delta V \sin(\omega_B t + \phi)$, $\Delta v_{SCb} = \Delta v_{SCc} = 0$), which results into

$$\langle \Delta v_{SCp} \rangle_1 (j\Omega) = \frac{\Delta V}{2\sqrt{3}j} e^{j\phi}$$

2) Balanced Case
   Here we consider balanced three phase perturbation in SSSC injected phase voltages (i.e. $\Delta v_{SCa} = \Delta V \sin(\omega_B t + \phi)$, $\Delta v_{SCb} = \Delta V \sin(\omega_B t - 2\pi/3 + \phi)$ and $\Delta v_{SCc} = \Delta V \sin(\omega_B t + 2\pi/3 + \phi)$). This scheme gives,

$$\langle \Delta v_{SCp} \rangle_1 (j\Omega) = \frac{\sqrt{3}\Delta V}{2j} e^{j\phi}$$

By substituting these results in (17) we get the same conclusion as in the previous cases.

IV. Simulation results with detailed models

In order to verify the results derived in previous section, digital simulation was carried out with detailed generator model using MATLAB/SIMULINK [11]. The test system is adapted from IEEE First Benchmark Model (FBM) [12]. The single line diagram of the system is shown Fig. 4 network parameters are also shown therein. The FBM has several closely spaced torsional modes and hence it is a good system to critically evaluate the SSR performance of a scheme. Mechanical (viscous) damping is considered for the test system and the coefficients for damping are taken as $D_{HP} = D_{IP} = D_{LPA} = D_{LPB} = 0.2$ pu torque/pu speed, $D_G = D_{EXC} = 0$ [2]. The maximum value of balanced fixed capacitor compensation which can be used is approximately $X_{FC} = 0.15$ pu, since any value higher than this causes the network mode to come close to a torsional mode and causes it to be unstable. This is evident from the eigenvalue analysis for two values of X_{FC} presented in Table-I. Torsional mode 5 is unaffected by the electrical network [2].

TABLE I
EIGEN VALUES OF THE SYSTEM : NO VARIABLE COMPENSATION

X_{FC} **= 0.15 pu**	X_{FC} **= 0.19 pu**	**Remarks**
-0.674$\pm j$9.099	-0.719$\pm j$9.377	Swing mode
-3.799$\pm j$219.65	-4.660$\pm j$200.76	Sub synch. network mode
-4.624$\pm j$533.82	-4.647$\pm j$553.51	Super synch. network mode
-0.145$\pm j$99.237	-0.144$\pm j$99.29	Torsional mode 1
-0.024$\pm j$127.03	-0.024$\pm j$127.04	Torsional mode 2
-0.304$\pm j$160.67	-0.297$\pm j$160.72	Torsional mode 3
0.017$\pm j$203.29	**1.021$\pm j$202.4**	Torsional mode 4 (**TM4** - Critical Mode)
-0.364$\pm j$298.18	-0.364$\pm j$298.18	Torsional mode 5

It is clear for the maximum feasible level of fixed series compensation, that torsional mode 4, denoted henceforth as '**TM4**', is the critical mode. If a larger value of overall compensation is desired, then it cannot be entirely in the form of fixed capacitor compensation but will require controlled compensation in the form of a TCSC or SSSC.

The case studies reported in this section focus on the SSR damping performance of the FACTS based schemes. The studies fall under the following categories:

1) Balanced and unbalanced schemes with fixed capacitor combined with a TCSC or a SSSC. The control schemes for a TCSC or a SSSC are rudimentary: fixed firing angle for a TCSC, and fixed reactive voltage injection for a SSSC. The aim of this study is to evaluate SSR mitigation due to detuning and passive damping effects.
2) The same study as above, except that the firing angle or injected voltage of a TCSC or SSSC respectively, is controlled by a SSR damping controller.

A. Simulation Studies with TCSC: Constant Firing Angle Control

We assume that the total steady state compensation in all phases due to a TCSC and fixed capacitor $(X_{FC} + X_{TCSC})$ is a constant. The balanced and unbalanced configurations are as shown in Fig. 1. Keeping this total steady state compensation unchanged, we do a parametric study for

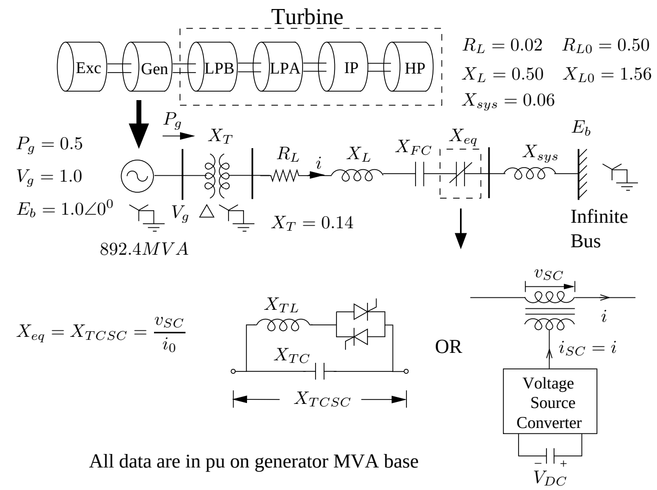

Fig. 4. IEEE First Benchmark Model (FBM)

1) Different firing angles keeping X_{TC} fixed, or
2) Different X_{TC} keeping the firing angle fixed.

It is expected that a TCSC will avoid SSR due to detuning effects; however this is a function of the TCSC sizing relative to X_{FC} and the firing angle of the TCSC [13] and is not generally true. For example, consider the situation if $X_{FC} = 0.15$ pu, $X_{TC} = 0.04$ pu, the ratio $\frac{\omega_n}{\omega_0} = \sqrt{\frac{X_{TC}}{X_{TL}}} = 2.8$, where ω_n is the natural resonance frequency of TCSC and ω_0 is the nominal system frequency in rad/s.

Note that the test disturbance is a step change in mechanical power of all the turbines which is applied at $t = 0.5s$. This excites all torsional modes and the electromechanical swing mode. Modal speed deviations are plotted to observe the effect of disturbance on individual modes separately. Note that in the simulation responses, the modal speed deviation $\Delta\omega_{Ml}$ corresponding to the mode "l" is approximately obtained as follows:

$$\Delta\omega_{Ml} = q_l^T [\Delta\omega_{HP} \quad \cdots \quad \Delta\omega_{Exc}]^T$$

where, q_l^T is a vector containing the left eigenvector components corresponding to individual angular speed deviations of the rotor masses of the turbine-generator system $(\Delta\omega_{HP} \quad \cdots \; \Delta\omega_{Exc})$.

If firing angle is $\alpha = 170^0$, then TM4 is unstable [14], which is observed in the modal speed deviations shown in Fig. 5, for the balanced case. However if the firing angle α is reduced, we can stabilize the torsional modes (see-Table-II).

The real parts of eigen value (decrement factors) corresponding to TM4 are shown to compare the effectiveness of the schemes. These values are calculated from the simulated responses of the modal speed. It is observed that for fixed firing angle control, the three phase scheme can stabilize the torsional mode-4 (TM4) when $\alpha = 155^0$ whereas the single phase scheme fails to stabilize the system. Modal speed deviations corresponding to TM4 with different firing angles for single phase and three phase schemes are shown in Figs. 6 and 7 respectively. These plots also highlight the same fact.

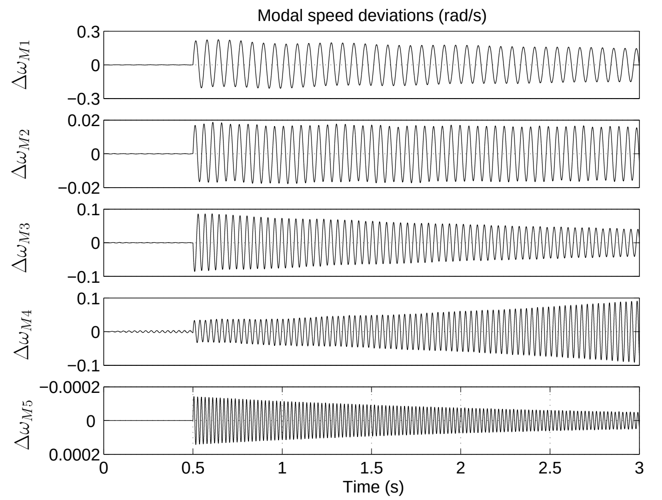

Fig. 5. Modal speed deviations for balanced scheme with TCSC ($\alpha = 170^0$)

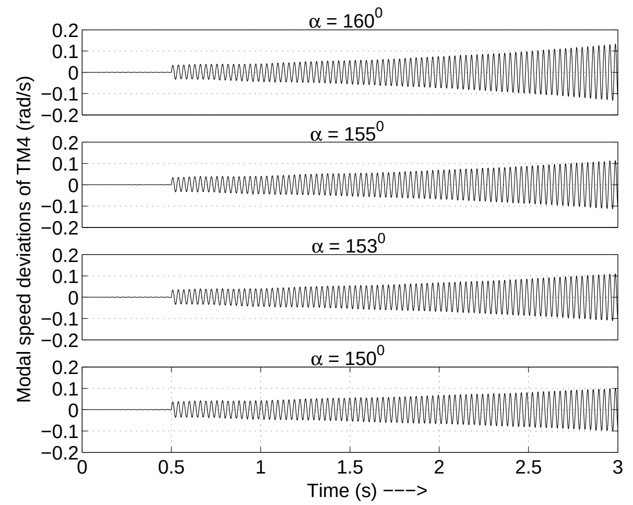

Fig. 6. Modal speed deviations of TM4 with TCSC (single phase scheme)

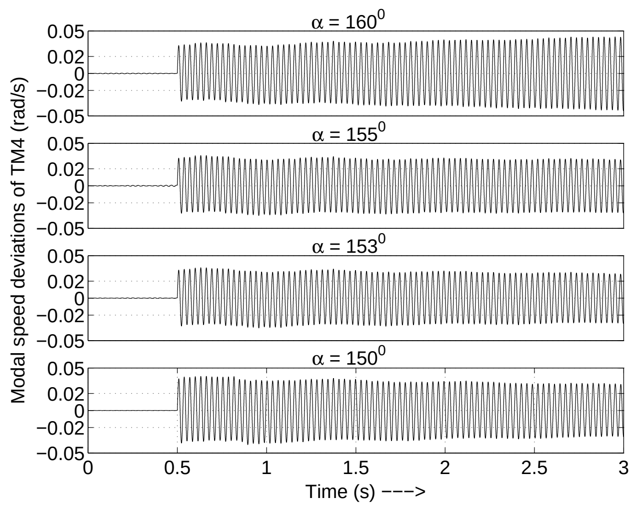

Fig. 7. Modal speed deviations of TM4 with TCSC (three phase scheme)

TABLE II
COMPARISON OF REAL PART OF EIGEN VALUES WITH FIXED X_{TC}

Firing angle (degree)	Reactance X_{TCSC} (pu)	Real part of eigenvalue (TM4) (Estimated from simulated responses)	
		Single phase scheme	Three phase scheme
160	0.049	0.555	0.104
155	0.067	0.486	-0.037
153	0.085	0.474	-0.075
150	0.179	0.406	-0.101
$X_{TC} = 0.04$ pu, $\omega_n/\omega_0 = 2.8$, $X_{FC} + X_{TCSC} = 0.191$ pu			

The schemes are evaluated with the firing angle of TCSC fixed and the value of X_{TC} is changed. As done in the previous cases, total series compensation i.e. $X_{FC} + X_{TCSC}$ is maintained constant for all the cases. The results corresponding to this approach are shown in Table-III. It can be concluded from the results that three phase scheme is more effective compared to single phase imbalance scheme for constant firing angle control. For a single phase TCSC, detuning effect obtained with constant firing angle control, cannot stabilize the unstable torsional mode.

TABLE III
COMPARISON OF REAL PART OF EIGEN VALUES WITH FIXED α

Blocked mode reactance X_{TC} (pu)	Reactance X_{TCSC} (pu)	Real part of eigenvalue (TM4) (Estimated from simulated responses)	
		Single phase scheme	Three phase scheme
0.04	0.049	0.555	0.104
0.045	0.055	0.542	0.065
0.06	0.074	0.498	0.013
0.08	0.098	0.476	-0.032
0.15	0.184	0.422	-0.095
$\alpha = 160^0$, $\omega_n/\omega_0 = 2.8$, $X_{FC} + X_{TCSC} = 0.191$ pu			

B. Simulation with SSSC: Fixed Reactive Voltage Injection

A SSSC [15] is implemented by a voltage source converter as shown in Fig. 1, which injects voltage in phase quadrature with the current. The net active power exchange with the line is only to compensate for the losses. The injected reactive voltage is regulated by controlling the phase angle of converter output voltages with respect to the line current. The modulation index of the controller is kept constant. The injected voltage is directly proportional to the DC side capacitor voltage. Any change in the reactive voltage is implemented by transiently changing the phase angle of the converter voltages, thereby changing the power drawn. This causes the capacitor voltage to change. This control strategy is often termed as Type II control [1]. An alternative control scheme (Type I - not used in this paper), keeps the capacitor voltage regulated by controlling the component in phase with the line current, but changes in the modulation index of the converter are used to effect changes in the injected voltage magnitude.

The following may be noted with reference to the simulations carried out with a SSSC in this paper:

1) Converter transformer is assumed to be ideal i.e. magnetizing branch is not modelled and the series reactance of transformer is assumed to be lumped with the line reactance.
2) Six pulse conversion is considered. The system reactance

TABLE IV
COMPARISON OF REAL PART OF EIGEN VALUES WITH SSSC

Injected voltage per phase (pu)	Real part of eigenvalue (TM4) (Estimated from simulated responses)	
	Single phase scheme	Three phase scheme
0.0142	0.412	0.011
0.0194	0.405	-0.035
0.0246	0.335	-0.055
0.0519	0.319	-0.068
$X_{FC} + \frac{v_{SC}}{i_0} = 0.191$ pu for all the cases		

provides adequate filtering action and the transmission line current is almost sinusoidal.

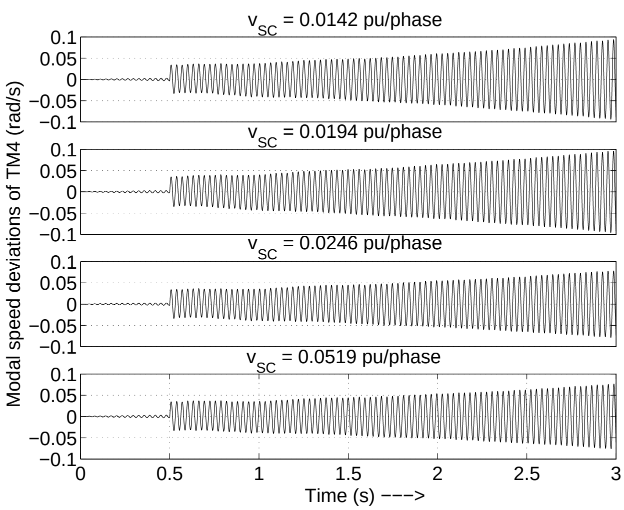

Fig. 8. Modal speed deviations of TM4 with SSSC (single phase scheme)

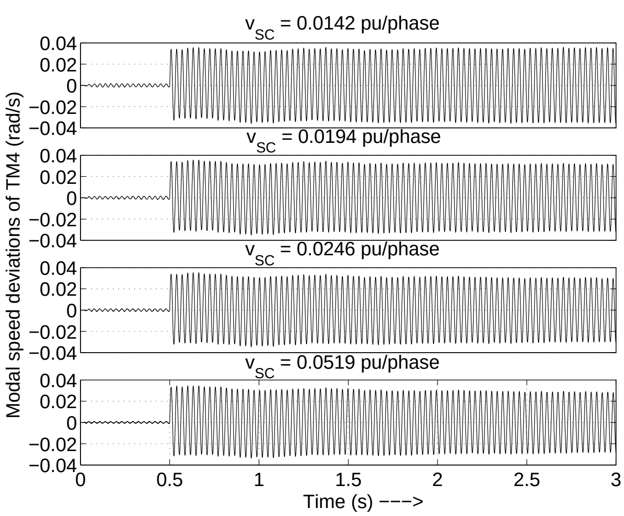

Fig. 9. Modal speed deviations of TM4 with SSSC (three phase scheme)

The reference value of voltage injected in series in each phase is computed such that it gives approximately the same series compensation as was given by TCSC with various firing angles as discussed in the previous system (i.e. $v_{SC} = i_0 X_{TCSC}$) where, i_0 is the line current magnitude in steady state. The variation of real part of eigen value for TM4 with SSSC is shown in Table-IV with different injected voltages. The three phase scheme is more effective in damping torsional oscillations compared to single phase scheme if injected voltage is constant. Variation in modal speed deviation for TM4 corresponding to single phase and three phase schemes with SSSC are shown in Figs. 8 and 9 respectively.

C. Simulation with TCSC and SSR Damping Controller

The rudimentary control strategies for a TCSC and SSSC discussed before, do not utilize the devices optimally. It is preferable to design a special damping controller for SSR. Output feedback control is preferred over state feedback for almost all power system controllers that are used in practice. Since complete pole placement is not feasible with output feedback control, the challenge in the design of such a damping controller is to prevent destabilization of any mode, while ensuring that the order of the controller transfer function is not impractically high. To compare and quantify the theoretical capabilities of the unbalanced and balanced schemes, it is appropriate to expend the control effort only on damping the mode of interest. If the feedback signal in which only the critical mode is observable is used, then it would serve our purpose without affecting other modes. Therefore the damping controllers utilize the critical modal speed as a feedback signal. The block diagram of the controller is shown in Fig 10. The controller design is based on damping torque analysis [16].

For roughly the same damping performance, the gain and controller effort is more (as expected) in the single phase TCSC or SSSC scheme. This manifests as a larger range

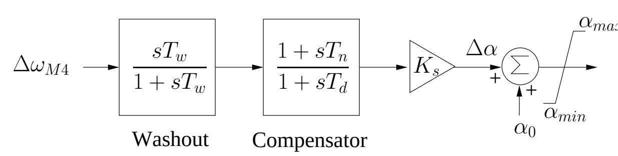

Fig. 10. Subsynchronous damping controller block diagram

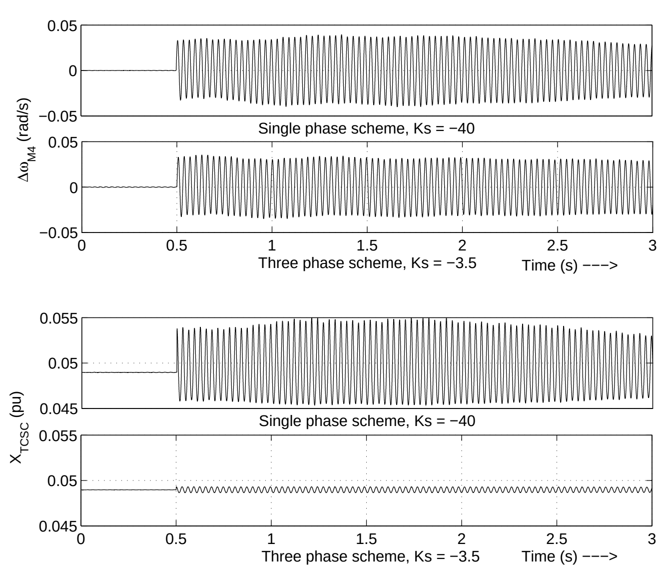

Fig. 11. Responses after a step change in mechanical torque alongwith TCSC and SSR damping controller: $\alpha_0 = 160^0$, $X_{TC} = 0.04$ pu, $T_w = 5$ s, $T_n = 0.05$ s, $T_d = 0.0002$ s

of variable compensation required to get the same damping performance for practical disturbances. This is evident from Fig. 11 which shows the modal speeds and X_{TCSC} with a step change in mechanical torque. Controller parameters are shown alongwith the responses. Similar results are obtained with SSSC.

Note that the single phase controller requires a much larger gain. This is not desirable in a practical controller, as larger gains have a tendency to destabilize unmodelled dynamics. Also, for controllers which utilize feedback signals in which other modes are observable, the order of the controller may be higher to ensure that the non-critical modes are not adversely affected by the higher required gains.

D. Simulation with SSSC and Power Swing Damping Controller

The Power Swing Damping Controller (PSDC) structure with a SSSC is shown in Fig. 12. The modal speed corresponding to the swing mode is used as the input signal. The total series compensation is taken as 0.15 pu. An Automatic Voltage Regulator (AVR) for the excitation system is modelled with a transfer function $\dfrac{K_A}{1+sT_A}$ and the gain and time constant are such that the swing mode is unstable.

The responses to the pulse disturbance in infinite bus voltage are shown in Fig. 13. It is observed here also that for almost

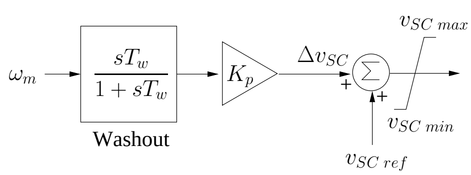

$$\omega_m = \frac{\omega_{HP}H_{HP} + \omega_{IP}H_{IP} + \cdots + \omega_{Exc}H_{Exc}}{H_{HP} + H_{IP} + \cdots + H_{Exc}}$$

Fig. 12. Power swing damping controller block diagram

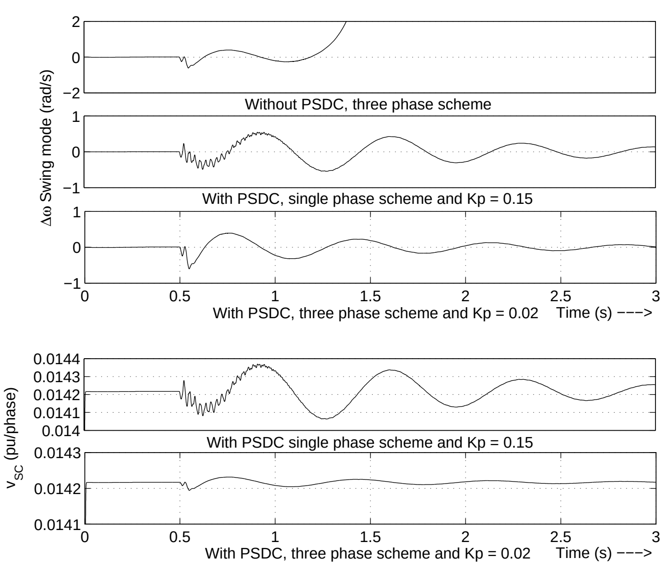

Fig. 13. Responses after a pulse change in infinite bus voltage with SSSC and Power Swing damping controller: $T_w = 5$ s, $K_A = 600, T_A = 0.006$ s, $v_{SC\ ref} = 0.0142$ pu/phase

the same damping performance, the required range of variable compensation and the gain is larger for single phase scheme.

V. Conclusion

An analytical evaluation of the performance of FACTS based phase imbalance schemes for damping torsional oscillations and power swings is presented in this paper. This analysis is facilitated by dynamic phasor modeling since it yields a time-invariant system of equations even for unbalanced three phase networks.

Simplified analysis indicates that the damping torque provided by a single phase imbalance scheme is one third of the three phase balanced scheme. Hence to achieve same damping performance, the control effort and gains needed with a single phase scheme will be much larger than an equivalent balanced scheme. The time domain simulation results support this. The results indicate that the cost and sizing requirements and controller design complexity of a single phase scheme will not be advantageous as compared to an equivalent balanced three phase scheme.

References

[1] K. R. Padiyar, *FACTS Controllers in Power Transmission and Distribution*. New Delhi, India: New Age Int., 2009.

[2] K. R. Padiyar, *Analysis of Subsynchronous Resonance in Power Systems*. Norwell, MA: Kluwer, 1999.

[3] N. G. Hingorani and L. Gyugyi, *Understanding FACTS*. New Delhi, India: Standard Publishers Distributors, 2001.

[4] A.-A. Edris, “Series compensation schemes reducing the potential of subsynchronous resonance,” *IEEE Trans. Power Syst.*, vol. 5, no. 1, pp. 219-226, Feb. 1990.

[5] A.-A. Edris, “Subsynchronous resonance countermeasure using phase imbalance,” *IEEE Trans. Power Syst.*, vol. 8, no. 4, pp. 1438-1447, Nov. 1993.

[6] M. C. Chudasama and A. M. Kulkarni, “Dynamic phasor analysis of SSR mitigation schemes based on passive phase imbalance,” *IEEE Trans. Power Syst.*, to be published.

[7] D. Rai, S.O. Faried, G. Ramakrishna, and A. -A. Edris, “Hybrid series compensation scheme capable of damping subsynchronous resonance,” *IET Gen. Trans. Distrib.*, vol. 4, no. 3, pp. 456-466, Mar. 2010.

[8] D. Rai, G. Ramakrishna, S. O. Faried, and A. -A. Edris, “Enhancement of power system dynamics using a phase imbalanced series compensation scheme,” *IEEE Trans. Power Syst.*, vol. 25, no. 2, pp. 966-974, May 2010.

[9] S. Subhash, B. N. Sarkar, and K. R. Padiyar, “A novel control strategy for TCSC to damp subsynchronous oscillations,” in *Proc. Seventh International Conference on AC-DC Power Transmission, 2001* (Conf. Publ. No. 485), Nov. 2001, pp. 181 - 186.

[10] A. M. Stankovic and T. Aydin, “Analysis of asymmetrical faults in power systems using dynamic phasors,” *IEEE Trans. Power Syst.*, vol. 15, no. 3, pp. 1062-1068, Aug. 2000.

[11] MATLAB and SIMULINK Demos and Documentation. [Online]. Available: http://www.mathworks.com/access/helpdesk/help/techdoc/.

[12] IEEE Subsynchronous Resonance Task Force, “First benchmark model for computer simulation of subsynchronous resonance,” *IEEE Trans. Power App. Syst.*, vol. PAS-96, no. 5, pp. 1565-1572, Sep. 1977.

[13] L.A.S. Pilotto, A. Bianco, W.F. Long and A.-A. Edris, “Impact of TCSC control methodologies on subsynchronous oscillations,” *IEEE Trans. Power Delivery*, vol 18, no. 1, pp. 243-252, Jan 2003.

[14] S. R. Joshi and A. M. Kulkarni, “Analysis of SSR performance of TCSC control schemes using a modular high bandwidth discrete-time dynamic model,” *IEEE Trans. Power Syst.*, vol. 24, no. 2, pp. 840-848, May 2009.

[15] L. Gyugyi, C. D. Schauder and K. K. Sen, “Static synchronous series compensator : A solid-state approach to the series compensation of transmission lines,” *IEEE Trans. Power Delivery*, vol. 12, no. 1, pp. 406-413, Jan 1997.

[16] S. R. Joshi, “Analysis of SSR performance of TCSC control schemes using discrete-time models,” Ph.D. dissertation, Dept. of Elect. Eng., Indian Institute of Technology, Bombay, India, 2010.